

# THE THEORETICAL PREDICTION FOR THE MUON ANOMALOUS MAGNETIC MOMENT

Michel Davier<sup>1</sup> and William J. Marciano<sup>2</sup>

<sup>1</sup>*Laboratoire de l'Accélérateur Linéaire, IN2P3-CNRS et Université de Paris-Sud, 91898 Orsay, France, email: davier@lal.in2p3.fr*

<sup>2</sup>*Brookhaven National Laboratory, Upton, New York 11973, email: marciano@bnl.gov*

**Key Words** quantum electrodynamics, electroweak theory, vacuum polarization, spectral functions

**PACS Codes** 11.00, 12.00

■ **Abstract** This article reviews the standard-model prediction for the anomalous magnetic moment of the muon and describes recent updates of QED, electroweak, and hadronic contributions. Comparison of theory and experiment suggests a  $2.4 \sigma$  difference if  $e^+e^- \rightarrow$  hadrons data are used to evaluate the main hadronic effects, but a smaller discrepancy if hadronic  $\tau$  decay data are employed. Implications of a deviation for “new physics” contributions, along with an outlook for future improvements in theory and experiment, are briefly discussed.

## CONTENTS

1. INTRODUCTION	116
2. QED CONTRIBUTIONS	119
3. ELECTROWEAK CONTRIBUTIONS	119
4. HADRONIC VACUUM POLARIZATION AT LOWEST ORDER	121
4.1. Outline of the Calculation	121
4.2. The Input Data from $e^+e^-$ Annihilation	123
4.3. The Input Data from $\tau$ Decays	125
4.4. Confronting $e^+e^-$ and $\tau$ Data	127
4.5. Special Cases	130
4.6. Results for the Leading-Order Hadronic Vacuum Polarization	131
4.7. Comparison of Different Analyses	132
5. HADRONIC THREE-LOOP EFFECTS	133
6. COMPARISON OF THEORY AND EXPERIMENT	134
7. NEW-PHYSICS CONTRIBUTIONS	136
8. OUTLOOK	137

## 1. INTRODUCTION

One of the great successes of the Dirac equation (1) was its prediction that the magnetic dipole moment,  $\vec{\mu}$ , of a spin  $|\vec{s}| = 1/2$  particle such as the electron (or muon) is given by

$$\vec{\mu}_l = g_l \frac{e}{2m_l} \vec{s}, \quad l = e, \mu, \dots, \quad 1.$$

with gyromagnetic ratio  $g_l = 2$ , a value already implied by early atomic spectroscopy. Later it was realized that a relativistic quantum field theory such as quantum electrodynamics (QED) can give rise via quantum fluctuations to a shift in  $g_l$ ,

$$a_l \equiv \frac{g_l - 2}{2}, \quad 2.$$

called the magnetic anomaly. In a now classic QED calculation, Schwinger (2) found the leading (one-loop) effect (Figure 1),

$$a_l = \frac{\alpha}{2\pi} \simeq 0.00116$$

$$\alpha \equiv \frac{e^2}{4\pi} \simeq 1/137.036. \quad 3.$$

This agreed beautifully with experiment (3), thereby providing strong confidence in the validity of perturbative QED. Today, we continue the tradition of testing QED and its  $SU(3)_C \times SU(2)_L \times U(1)_Y$  standard-model (SM) extension (which includes strong and electroweak interactions) by measuring  $a_l^{\text{exp}}$  for the electron and muon ever more precisely and comparing these measurements with  $a_l^{\text{SM}}$  expectations, calculated to much higher order in perturbation theory. Such comparisons test

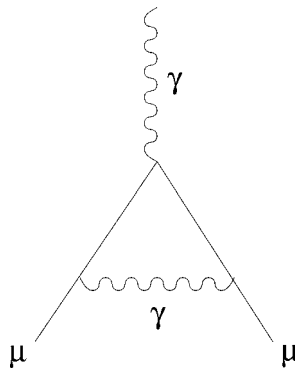


**Figure 1** The first-order QED correction to  $g=2$  of the muon.

the validity of the standard model and probe for “new physics” effects, which, if present in quantum-loop fluctuations, should cause disagreement at some level.

For the electron and positron (expected to have the same  $a_e$  if CPT symmetry holds), a series of Nobel-winning experiments by Dehmelt and collaborators (4) found

$$\begin{aligned} a_{e^-}^{\text{exp}} &= 0.0011596521884(43), \\ a_{e^+}^{\text{exp}} &= 0.0011596521879(43), \end{aligned} \tag{4}$$

where the bracketed number denotes the uncertainty in the last two significant figures. Those results are to be compared with the standard-model prediction (5, 6)

$$\begin{aligned} a_e^{\text{SM}} &= \frac{\alpha}{2\pi} - 0.328478444 \left(\frac{\alpha}{\pi}\right)^2 + 1.181234 \left(\frac{\alpha}{\pi}\right)^3 \\ &\quad - 1.7502 \left(\frac{\alpha}{\pi}\right)^4 + 1.7 \times 10^{-12}. \end{aligned} \tag{5}$$

The last, very small term stems from strong (hadronic) and electroweak quantum corrections (7), which are of order  $\sim(\alpha/\pi)^2(m_e/m_\rho)^2 \simeq 2 \times 10^{-12}$  and  $\sim(\alpha/\pi)(m_e/m_W)^2 \simeq 10^{-13}$ , respectively.

Comparison of Equations 4 and 5 yields the most precise determination of the fine structure constant (8):

$$\alpha^{-1} = 137.03599877(40). \tag{6}$$

The agreement of that value with the more direct (but less precise) measurements (9) of  $\alpha$ ,

$$\begin{aligned} \alpha^{-1} &= 137.03600300(270) && \text{[Quantum Hall]}, \\ \alpha^{-1} &= 137.03600840(330) && \text{[Rydberg } (h/m_n)\text{]}, \\ \alpha^{-1} &= 137.03598710(430) && \text{[AC Josephson]}, \\ \alpha^{-1} &= 137.03599520(790) && \text{[Muonium HFS]}, \end{aligned} \tag{7}$$

confirms the validity of QED to a precision of  $3 \times 10^{-8}$ . That agreement, along with other precision studies, makes QED the best theory in physics. An experiment under way at Harvard (10) aims to improve the measurement of  $a_e$  by about a factor of 15. Combined with a much improved independent determination of  $\alpha$ , it would significantly test the validity of perturbative QED (11). It should be noted, however, that  $a_e$  is in general not very sensitive to “new physics” at a high mass scale  $\Lambda$  because its effect on  $a_e$  is expected (12) to be quadratic in  $1/\Lambda$ :

$$\Delta a_e(\Lambda) \sim \mathcal{O}\left(\frac{m_e^2}{\Lambda^2}\right). \tag{8}$$

Hence, the effect is expected to be highly suppressed by the smallness of the electron mass.  $a_e$  would be much more sensitive if  $\Delta a_e$  were linear in  $1/\Lambda$ ; but that is unlikely if chiral symmetry is present in the  $m_e \rightarrow 0$  limit.

The muon magnetic anomaly has recently been measured with a precision of  $5 \times 10^{-7}$  by the E821 collaboration at Brookhaven National Laboratory (13).

$$\begin{aligned} a_{\mu^+}^{\text{exp}} &= 116592030(80) \times 10^{-11}, \\ a_{\mu^-}^{\text{exp}} &= 116592140(85) \times 10^{-11}, \quad \text{and} \\ a_{\mu}^{\text{exp}} &= 116592080(58) \times 10^{-11} \quad [\text{average}]. \end{aligned} \quad 9.$$

Although the accuracy is 200 times worse than  $a_e^{\text{exp}}$ ,  $a_{\mu}$  is about  $m_{\mu}^2/m_e^2 \simeq 40,000$  times more sensitive to “new physics” and hence a better place (by about a factor of 200) to search for a deviation from standard-model expectations. Of course, strong and electroweak contributions to  $a_{\mu}$  are also enhanced by  $m_{\mu}^2/m_e^2 \simeq 40,000$  relative to  $a_e$ , so they must be evaluated much more precisely in any meaningful comparison of  $a_{\mu}^{\text{SM}}$  with Equation 9. Fortunately, the recent experimental progress in  $a_{\mu}^{\text{exp}}$  has stimulated much theoretical improvement of  $a_{\mu}^{\text{SM}}$ , uncovering errors and inspiring new computational approaches along the way.

The theoretical prediction for  $a_{\mu}^{\text{SM}}$  is generally divided into three contributions,

$$a_{\mu}^{\text{SM}} = a_{\mu}^{\text{QED}} + a_{\mu}^{\text{EW}} + a_{\mu}^{\text{hadronic}}, \quad 10.$$

and each has undergone and continues to be subjected to detailed scrutiny. The QED contribution has been computed through four loops (i.e.,  $\mathcal{O}(\alpha/\pi)^4$ ) and estimated at the five-loop level. A recent revision (14) of the  $(\alpha/\pi)^4$  contribution (described in Section 2) has shifted the prediction for  $a_{\mu}^{\text{QED}}$  upward by about  $15 \times 10^{-11}$ . Electroweak corrections have been computed at the one- and two-loop levels (15) (see Section 3). In fact,  $a_{\mu}^{\text{EW}}$  represents the first full two-loop electroweak standard-model calculation. Hadronic (i.e., strong interaction) effects from low-energy quark and gluon loop effects have been evaluated at order  $(\alpha/\pi)^2$  and  $(\alpha/\pi)^3$  using  $e^+e^- \rightarrow$  hadrons data via a dispersion relation and employing hadronic  $\tau$  decays as a consistency check. At the three-loop level in  $\alpha$ , the so-called hadronic light-by-light (LBL) contributions must be estimated in a model-dependent approach. Those estimates have been plagued by errors, which now seem to be sorted out. Nevertheless, the remaining overall uncertainties from hadronic vacuum polarization and LBL in  $a_{\mu}^{\text{hadronic}}$  represent the main theoretical error in  $a_{\mu}^{\text{SM}}$ . Its current status is reviewed in Sections 4 and 5.

In the remainder of this review, we describe the updates of QED, electroweak, and hadronic contributions mentioned above, with particular emphasis on hadronic effects where the uncertainty is most problematic. We then compare (in Section 6)  $a_{\mu}^{\text{exp}}$  with  $a_{\mu}^{\text{SM}}$  and show that a  $2.4 \sigma$  difference exists, using the estimate of  $a_{\mu}^{\text{hadronic}}$  from  $e^+e^-$  data. The implications of a deviation (if real) for “new physics” such as supersymmetry, extra dimensions, or dynamical supersymmetry breaking are very briefly outlined in Section 7. Section 8 considers possible future improvements in  $a_{\mu}$  theory and experiment.

## 2. QED CONTRIBUTIONS

The QED contributions to  $a_\mu^{\text{SM}}$  start with  $\alpha/2\pi$  from the Schwinger (2) one-loop diagram in Figure 1 and include higher-order extensions obtained by adding photon lines and closed lepton loops ( $l = e, \mu, \tau$ ). Those contributions have been fully evaluated through four loops, and the leading five-loop effects [enhanced by  $\ln(m_\mu/m_e) \sim 5.3$  factors] have been estimated (5, 6, 14, 16). Currently one finds

$$a_\mu^{\text{QED}} = \frac{\alpha}{2\pi} + 0.765857376 \left(\frac{\alpha}{\pi}\right)^2 + 24.05050898 \left(\frac{\alpha}{\pi}\right)^3 + 131.0 \left(\frac{\alpha}{\pi}\right)^4 + 930 \left(\frac{\alpha}{\pi}\right)^5, \quad 11.$$

which, for the value of  $\alpha$  in Equation 6, leads to

$$a_\mu^{\text{QED}} = 116584720.7(0.4)(1) \times 10^{-11}. \quad 12.$$

That result is somewhat larger (by about  $15 \times 10^{-11}$ ) than earlier predictions. This is due to an update in the  $(\frac{\alpha}{\pi})^4$  coefficient from 126 to a (preliminary) value of 131.0 reported by Kinoshita (14), and, to a lesser extent, to the small increase in  $\alpha$  (see Equation 6). The quoted errors in Equation 12 stem from the uncertainties in  $\alpha$  and the five-loop QED estimate.

It is often noted that the coefficients in Equation 11 are all positive and growing, whereas the coefficients in  $a_e^{\text{SM}}$  (see Equation 5) are better behaved, i.e., all of  $O(1)$  and alternate in sign. That difference arises from electron vacuum polarization effects in  $a_\mu^{\text{QED}}$  [i.e., relatively large  $\ln(m_\mu/m_e)$  contributions] and the unusually large contribution from the LBL scattering electron loop (16), which provides about 21/24 of the  $\mathcal{O}(\alpha/\pi)^3$  coefficient. Once that coefficient turned out to be large and positive, the higher-order coefficients were destined to be large and positive via electron vacuum polarization insertions in the LBL amplitudes. So the growing magnitude of the coefficients is well understood and not indicative of a breakdown in perturbation theory.

## 3. ELECTROWEAK CONTRIBUTIONS

Loop contributions to  $a_\mu^{\text{SM}}$  involving heavy  $W^\pm$ , Z, or Higgs particles are collectively labeled as  $a_\mu^{\text{EW}}$ . They are generically suppressed by a factor  $(\alpha/\pi)(m_\mu/m_W)^2 \simeq 4 \times 10^{-9}$  but are nevertheless within the sensitivity range of the E821 experiment (13). The one-loop contributions to  $a_\mu^{\text{EW}}$  illustrated in Figure 2 were computed more than 30 years ago (17), primarily to test their finiteness (as required for renormalizability). Those studies found

$$a_\mu^{\text{EW}, 1\text{-loop}} = \frac{G_\mu m_\mu^2}{8\sqrt{2}\pi^2} \left[ \frac{5}{3} + \frac{1}{3}(1-4\sin^2\theta_W)^2 + \mathcal{O}\left(\frac{m_\mu^2}{m_W^2}\right) + \mathcal{O}\left(\frac{m_\mu^2}{m_H^2}\right) \right]$$

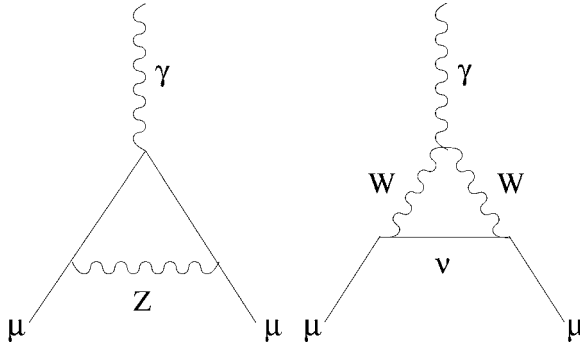


**Figure 2** The two most important first-order electro-weak contributions.

$$G_\mu = \frac{g^2}{4\sqrt{2}m_W^2} = 1.16637(1) \times 10^{-5} \text{ GeV}^{-2}$$

$$\sin^2 \theta_W = 1 - m_W^2/m_Z^2 = 0.223 \quad (\text{for } m_H = 150 \text{ GeV}) \quad 13.$$

or

$$a_\mu^{\text{EW},1\text{-loop}} = 194.8 \times 10^{-11}. \quad 14.$$

Interest in the two-loop contribution to  $a_\mu^{\text{EW}}$  began with the observation (18) that some two-loop electroweak diagrams containing photons and heavy weak bosons were enhanced by relatively large logs,  $\ln(m_Z^2/m_\mu^2) \simeq 13.5$ , relative to naive expectations. Later, the complete two-loop calculation, including both logs and non-log parts, was completed (15). Contributions enhanced by  $\ln(m_Z/m_\mu)$  or  $\ln(m_Z/m_f)$  ( $m_f = \text{fermion mass} \ll m_Z$ ), called leading logs (LL), were recently updated and found to be (19)

$$a_\mu^{\text{EW},2\text{-loop,LL}} = -34.7(1.0) \times 10^{-11}. \quad 15.$$

All other contributions, collectively called non-leading logs (NLL), give (15)

$$a_\mu^{\text{EW},2\text{-loop,NLL}} = -6.0(1.8) \times 10^{-11}. \quad 16.$$

The uncertainty in Equation 15 comes from hadronic effects in the quark triangle diagrams of Figure 3, whereas the error in Equation 16 stems mainly from the Higgs mass uncertainty. Together, they give

$$a_\mu^{\text{EW}} = -40.7(1.0)(1.8) \times 10^{-11}, \quad 17.$$

or, combined with Equation 14,

$$a_\mu^{\text{EW}} = 154(1)(2) \times 10^{-11}. \quad 18.$$

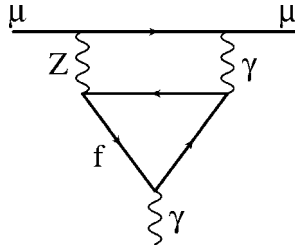


**Figure 3** An example of a two-loop electroweak contribution (triangle diagram).

The 21% reduction of the one-loop result is surprisingly large. Hence, it was important to evaluate the leading-log three-loop effects of the form  $G_\mu m_\mu^2 (\alpha/\pi)^2 [\ln(m_Z/m_\mu)]^2$  via a renormalization group analysis. Such an analysis (19, 20) found those effects to be negligible,  $O(10^{-12})$ .

Among the novel features of the full two-loop electroweak calculation, the fermion triangle diagrams (Figure 3) are perhaps the most interesting. They are individually divergent for a given fermion due to the Adler-Bell-Jackiw (ABJ) anomaly (21). Those divergencies cancel when summed over a complete generation of quarks and leptons. However, the low-loop-momentum region does not fully cancel owing to different fermion masses and strong interaction effects. Therefore, one needs to carefully evaluate the light quark contributions in a manner that respects the short-distance quark properties (which are not renormalized by strong interactions) (19) but at the same time preserves (22) the chiral properties of the massless quark limit,  $m_u = m_d = 0$ . Such an analysis was carried out (19) utilizing the operator product expansion, and its detailed numerical results are included in Equation 17. It was observed in that study that a constituent quark mass calculation (15) with  $m_u = m_d = 300 \text{ MeV}$  and  $m_s = 500 \text{ MeV}$  combined with the pion pole contribution (22) (avoiding short-distance double counting) reproduces very accurately the results of a much more detailed hadronic model calculation (17). Such an approach is also useful for the LBL contribution to  $a_\mu^{\text{hadronic}}$ , which is discussed in Section 5.

## 4. HADRONIC VACUUM POLARIZATION AT LOWEST ORDER

### 4.1. Outline of the Calculation

Unlike the QED part, the contribution from hadronic polarization in the photon propagator (Figure 4) cannot currently be computed from theory alone, because most of the contributing hadronic physics occurs in the low-energy nonperturbative QCD regime. However, by virtue of the analyticity of the vacuum polarization

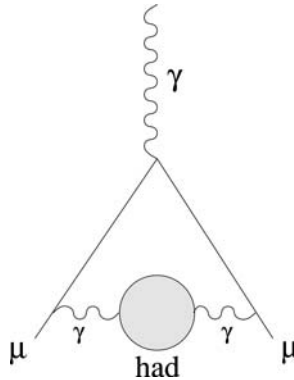


**Figure 4** The lowest-order hadronic contribution.

correlator, the contribution of the hadronic vacuum polarization to  $a_\mu$  can be calculated via the dispersion integral (23)

$$a_\mu^{\text{had,LO}} = \frac{\alpha^2(0)}{3\pi^2} \int_{4m_\mu^2}^{\infty} ds \frac{K(s)}{s} R(s), \quad 19.$$

where  $K(s)$  is the QED kernel (24),

$$K(s) = x^2 \left(1 - \frac{x^2}{2}\right) + (1+x)^2 \left(1 + \frac{1}{x^2}\right) \left(\ln(1+x) - x + \frac{x^2}{2}\right) + \frac{(1+x)}{(1-x)} x^2 \ln x, \quad 20.$$

with  $x = (1 - \beta_\mu)/(1 + \beta_\mu)$  and  $\beta_\mu = (1 - 4m_\mu^2/s)^{1/2}$ . In Equation 19,  $R(s) \equiv R^{(0)}(s)$  denotes the ratio of the “bare” cross section for  $e^+e^-$  annihilation into hadrons to the lowest-order muon-pair-production cross section. The “bare” cross section is defined as the measured cross section, corrected for initial-state radiation, electron-vertex loop contributions, and vacuum polarization effects in the photon propagator. The reason for using the “bare” (i.e., lowest-order) cross section is that a full treatment of higher orders is needed anyhow at the level of  $a_\mu$ , so the use of “dressed” cross sections would entail the risk of double-counting some of the higher-order contributions, or in some cases might actually incorrectly evaluate some of the higher-order contributions.

The function  $K(s)$  decreases monotonically with increasing  $s$ . It gives a strong weight to the low-energy part of the integral in Equation 19. About 91% of the total contribution to  $a_\mu^{\text{had,LO}}$  is accumulated at center-of-mass energies  $\sqrt{s}$  below 1.8 GeV, and 73% of  $a_\mu^{\text{had,LO}}$  is covered by the two-pion final state, which is dominated by the  $\rho(770)$  resonance.



Many calculations of the hadronic vacuum polarization contribution have been carried out in the past, taking advantage of the  $e^+e^-$  data available at that time. The results depend crucially on the quality of the input data, which has been improving with better detectors and higher-luminosity machines. Therefore, the later calculations, with more complete and better-quality data, supersede the results of the former ones. In addition, some approaches make use of theory constraints, not only in the high-energy region where perturbative QCD applies (25–27), but also at lower energy (28, 29). Also, it was proposed (30) that data on hadronic  $\tau$  decays could be used to extract the relevant spectral functions, with greater precision than was possible using the  $e^+e^-$  data available then.

In this review, we follow the latest published analysis by Davier, Eidelman, Höcker, & Zhang (DEHZ) (31), which considers both  $e^+e^-$  and  $\tau$  input. We then present comparisons with other independent approaches.

## 4.2. The Input Data from $e^+e^-$ Annihilation

**4.2.1. THE MEASUREMENTS** The exclusive low-energy  $e^+e^-$  cross sections have been mainly measured by experiments running at  $e^+e^-$  colliders in Novosibirsk and Orsay. Because of the higher hadron multiplicity at energies above  $\sim 2.5$  GeV, the exclusive measurement of the many hadronic final states is not practicable. Consequently, the experiments at the high-energy colliders ADONE, SPEAR, DORIS, PETRA, PEP, VEPP-4, CESR, and BEPC have measured the total inclusive cross section ratio  $R$ . Complete references to published data are given in Reference (32).

The most precise  $e^+e^- \rightarrow \pi^+\pi^-$  measurements come from CMD-2. These are now available in their final form (33), after a significant revision that fixed problems relating to radiative corrections. The results are corrected for leptonic and hadronic vacuum polarization and for photon radiation by the pions (final-state radiation—FSR), so that the measured final state corresponds to  $\pi^+\pi^-$ , including pion-radiated photons and virtual final-state QED effects. The overall systematic error of the final data is quoted to be 0.6% and is dominated by the uncertainties in the radiative corrections (0.4%).

The comparison between the cross-section results from CMD-2 and from previous experiments (corrected for vacuum polarization and FSR, according to the procedure discussed in Section 4.2.2) shows agreement within the much larger uncertainties (2–10%) quoted by the older experiments. But the new CMD-2 results only cover the energy range from 0.61 to 0.96 GeV, so the older data must still be relied on below and above these values.

Among other exclusive channels with important contributions, the process  $e^+e^- \rightarrow \pi^+\pi^-\pi^0\pi^0$  shows rather large discrepancies among different experiments. Some measurements are incomplete, as in the case of  $e^+e^- \rightarrow K\bar{K}\pi\pi$  or  $e^+e^- \rightarrow 6\pi$ , and one has to rely on isospin symmetry to estimate or bound the unmeasured cross sections.

**4.2.2. RADIATIVE CORRECTIONS TO  $e^+e^-$  DATA** The evaluation of the integral in Equation 19 requires the use of the “bare” hadronic cross section, so the input data

must be analyzed with care in this respect. Three steps are to be considered in the radiative correction procedure:

- The hadronic cross sections given by the experiments are always corrected for initial-state radiation and the effect of loops at the electron vertex.
- The vacuum polarization correction in the photon propagator is a more delicate point. The cross sections need to be corrected, i.e.,

$$\sigma_{\text{bare}} = \sigma_{\text{dressed}} \left( \frac{\alpha(0)}{\alpha(s)} \right)^2, \quad 21.$$

where  $\sigma_{\text{dressed}}$  is the measured cross section already corrected for initial-state radiation, and  $\alpha(s)$  takes into account leptonic and hadronic vacuum polarization. The new data from CMD-2 (33) are explicitly corrected for both leptonic and hadronic vacuum polarization effects (the latter involving an iterative procedure), whereas data from older experiments in general were not.

In fact, what really matters is the correction to the ratio of the hadronic cross section to the cross section for the process used for the luminosity determination. Generally, the normalization is done with respect to large-angle Bhabha scattering events. In the  $\pi^+\pi^-$  mode, all experiments before the latest CMD-2 results corrected their measured processes ( $\pi^+\pi^-$ ,  $\mu^+\mu^-$ , and  $e^+e^-$ ) for radiative effects using  $O(\alpha^3)$  calculations that took only leptonic vacuum polarization into account (34, 35). For those older experiments, a correction  $C_{\text{HVP}}$  is applied for the missing hadronic vacuum polarization (36):

$$C_{\text{HVP}} = \frac{1 - 2\Delta\alpha_{\text{had}}(s)}{1 - 2\Delta\alpha_{\text{had}}(\bar{t})}, \quad 22.$$

where the correction in the denominator applies to the Bhabha cross section evaluated at a mean value of the squared momentum transfer  $t$ , which depends on the angular acceptance in each experiment. A 50% uncertainty is assigned to  $C_{\text{HVP}}$ .

- In Equation 19,  $R(s)$  must include the contribution of all hadronic states produced at the energy  $\sqrt{s}$ . In particular, it must include those with FSR. Investigating the existing data in this respect is also a difficult task. In the  $\pi^+\pi^-$  data from CMD-2 (33), most additional photons are experimentally rejected to reduce backgrounds from other channels, and the fraction kept is subtracted using the Monte Carlo simulation that includes a model for FSR. Then the full FSR contribution is added back as a correction,  $C_{\text{FSR}}$ , using an analytical expression computed using scalar QED (point-like pions) (37). Because this effect was not included in earlier analyses, the same correction is applied to older  $\pi^+\pi^-$  data and assigned a 100% uncertainty.

The different corrections in the  $\pi^+\pi^-$  contribution amount to  $-2.3\%$  for leptonic vacuum polarization,  $+0.9\%$  for hadronic vacuum polarization, and  $+0.9\%$  for FSR. The correction  $C_{\text{HVP}}$  is small, typically  $0.56\%$ .

### 4.3. The Input Data from $\tau$ Decays

4.3.1. SPECTRAL FUNCTIONS FROM  $\tau$  DECAYS Data from  $\tau$  decays into two- and four-pion final states  $\tau^- \rightarrow \nu_\tau \pi^- \pi^0$ ,  $\tau^- \rightarrow \nu_\tau \pi^- 3\pi^0$ , and  $\tau^- \rightarrow \nu_\tau 2\pi^- \pi^+ \pi^0$  are available from ALEPH (38), CLEO (39, 40), and OPAL (41). Recently, ALEPH has presented preliminary results on the full LEP1 statistics (42).

Assuming (for the moment) isospin invariance to hold, the corresponding  $e^+e^-$  isovector cross sections are calculated via the conserved vector current (CVC) relations

$$\sigma_{e^+e^- \rightarrow \pi^+\pi^-}^{I=1} = \frac{4\pi\alpha^2}{s} v_{\pi^-\pi^0}, \quad (23)$$

$$\sigma_{e^+e^- \rightarrow \pi^+\pi^-\pi^+\pi^-}^{I=1} = 2 \cdot \frac{4\pi\alpha^2}{s} v_{\pi^-3\pi^0}, \quad (24)$$

$$\sigma_{e^+e^- \rightarrow \pi^+\pi^-\pi^0\pi^0}^{I=1} = \frac{4\pi\alpha^2}{s} [v_{2\pi^-\pi^+\pi^0} - v_{\pi^-3\pi^0}]. \quad (25)$$

The  $\tau$  spectral function  $v_V(s)$  for a given vector hadronic state  $V$  is defined by (43)

$$v_V(s) \equiv \frac{m_\tau^2}{6|V_{ud}|^2 S_{EW}} \frac{B(\tau^- \rightarrow \nu_\tau V^-)}{B(\tau^- \rightarrow \nu_\tau e^- \bar{\nu}_e)} \frac{dN_V}{N_V ds} \left[ \left(1 - \frac{s}{m_\tau^2}\right)^2 \left(1 + \frac{2s}{m_\tau^2}\right) \right]^{-1}, \quad (26)$$

where  $|V_{ud}| = 0.9748 \pm 0.0010$  is obtained from averaging the determinations (44) from nuclear  $\beta$  decays and kaon decays (assuming unitarity of the CKM matrix), and  $S_{EW}$  accounts for electroweak radiative corrections as discussed in Section 4.3.2. The spectral function are obtained from the corresponding invariant mass distributions by subtracting out the non- $\tau$  background and the feedthrough from other  $\tau$  decay channels, after a final unfolding from detector response. Note that the measured  $\tau$  spectral function are inclusive with respect to radiative photons.

It should be pointed out that the experimental conditions for studying  $\tau$  decays at the  $Z$  pole (ALEPH, OPAL) and at the  $\Upsilon(4S)$  (CLEO) energies are very different. On the one hand, at LEP, the  $\tau^+\tau^-$  events can be selected with high efficiency ( $>90\%$ ) and small non- $\tau$  background ( $<1\%$ ), thus ensuring little bias in the efficiency determination. Despite higher background and smaller efficiency, CLEO has the advantage of lower energy for the reconstruction of the decay final state, since particles are more separated in space. One can therefore consider ALEPH/OPAL and CLEO data to be approximately uncorrelated as far as experimental procedures are concerned. The fact that their respective spectral functions for the  $\pi^-\pi^0$  and  $2\pi^-\pi^+\pi^0$  modes agree is therefore a valuable experimental consistency test.

4.3.2. ISOSPIN SYMMETRY BREAKING The relationships shown in Equations 23, 24, and 25 between  $e^+e^-$  and  $\tau$  spectral functions only hold in the limit of exact isospin

invariance. They follow from the factorization of strong-interaction physics as produced through the  $\gamma$  and  $W$  propagators out of the QCD vacuum. However, symmetry breaking is expected at some level from electromagnetic processes, whereas the small  $u, d$  mass splitting leads to negligible effects. Various identified sources of isospin breaking are considered in the dominant  $2\pi$  channel.

- Electroweak radiative corrections yield their dominant contribution from the short-distance correction to the effective four-fermion coupling  $\tau^- \rightarrow \nu_\tau(d\bar{u})^-$ , enhancing the  $\tau$  amplitude by the factor  $(1 + 3\alpha(m_\tau)/4\pi)(1 + 2\bar{Q}) \ln(M_Z/m_\tau)$ , where  $\bar{Q}$  is the average charge of the final-state partons (45, 46). Although this correction vanishes for leptonic decays, it contributes for quarks. All higher-order logarithms can be resummed using the renormalization group (45, 47) into an overall multiplicative electroweak factor  $S_{EW}^{\text{had}}$ , which is equal to 1.0194. The difference between the resummed value and the lowest-order estimate (1.0188) can be taken as a conservative estimate of the uncertainty. QCD corrections to  $S_{EW}^{\text{had}}$  have been calculated (45, 46) and found to be small, reducing its value to 1.0189. Subleading non-logarithmic short-distance corrections have been calculated to order  $\alpha$  for the leptonic width (45),  $S_{EW}^{\text{sub,lep}} = 1 + \alpha(25/4 - \pi^2)/2\pi \simeq 0.9957$ .
- A contribution (30, 48) for isospin breaking occurs because of the mass difference between charged and neutral pions, which is essentially of electromagnetic origin. The spectral function has a kinematic factor  $\beta^3$  that is different in  $e^+e^- (\pi^+\pi^-)$  and  $\tau$  decay ( $\pi^-\pi^0$ ),

$$v_{0,-}(s) = \frac{\beta_{0,-}^3(s)}{12} |F_{\pi^0,-}^{0,-}(s)|^2, \quad 27.$$

$F_{\pi^0,-}^{0,-}(s)$  being the electromagnetic and weak pion form factors, respectively, where  $\beta_{0,-} = \beta(s, m_{\pi^-}, m_{\pi^0})$  is given in Reference (32).

- Other corrections occur in the form factor itself. It is affected by the pion mass difference because the same  $\beta^3$  factor enters in the  $\rho \rightarrow \pi\pi$  width. This effect partially compensates the  $\beta^3$  correction (Equation 27) of the cross section. Similarly, mass and width differences between the charged and neutral  $\rho$  meson (30, 49, 50) will affect the resonance lineshape, which can however be studied directly by using the measured spectral functions.
- $\rho - \omega$  interference occurs in the  $\pi^+\pi^-$  mode only, but its contribution can be readily introduced into the  $\tau$  spectral function using the parameters determined in the CMD-2 fit (33). Also, electromagnetic decays explicitly break SU(2) symmetry for the  $\rho$  width. This is the case for the decays  $\rho \rightarrow \pi\pi^0\gamma$ ,  $\pi\gamma$  and  $\rho^0 \rightarrow \eta\gamma, l^+l^-$ . Calculations have been done for the decay  $\rho \rightarrow \pi\pi\gamma$  with an effective model (51).
- Long-distance corrections are expected to be final-state dependent in general. A consistent calculation of radiative corrections for the  $\nu_\tau\pi^-\pi^0$  mode has been recently performed and includes the effect of loops (52, 53). The  $\tau$

spectral function must be divided by a factor  $S_{EW}^{\pi\pi^0}(s)$ ,

$$S_{EW}^{\pi\pi^0}(s) = \frac{S_{EW}^{\text{had}} G_{EM}(s)}{S_{EW}^{\text{sub,lep}}} = (1.0233 \pm 0.0006) \cdot G_{EM}(s), \quad 28.$$

where  $G_{EM}(s)$  is the long-distance radiative correction, which involves both real photon emission and virtual loops. The form factor correction is dominated by the effect of the pion mass difference in the  $\rho$  width, so that the correction is rather independent from the chosen parameterization of the form factor.

Finally, the total correction to  $a_\mu^{\text{hadronic}}$  from isospin breaking amounts to  $(-93 \pm 24) 10^{-11}$  when the  $\tau 2\pi$  data are used.

#### 4.4. Confronting $e^+e^-$ and $\tau$ Data

The new  $e^+e^-$  and the isospin-breaking corrected  $\tau$  spectral function can be directly compared for the  $\pi\pi$  final state. The  $\tau$  spectral function is obtained by averaging ALEPH (38), CLEO (39), and OPAL (41) results (32). The  $e^+e^-$  data are plotted as a point-by-point ratio to the  $\tau$  spectral function in Figure 5. The central bands in Figure 5 give the quadratic sum of the statistical and systematic errors of the  $\tau$  spectral function obtained by combining all  $\tau$  data. The  $e^+e^-$  and  $\tau$  data are consistent below and around the  $\rho$  peak, whereas a discrepancy persists for energies larger than 0.85 GeV. Part of the discrepancy could originate from different masses and widths for the neutral and charged  $\rho$ 's, but correcting for this effect spreads the disagreement over a wider mass range (49, 57).

A convenient way to assess the compatibility between  $e^+e^-$  and  $\tau$  spectral function evaluates the  $\tau$  decay fractions using the relevant  $e^+e^-$  spectral function as input. This procedure provides a quantitative comparison using a single number. Employing the branching fraction  $B(\tau^- \rightarrow \nu_\tau e^- \bar{\nu}_e) = (17.810 \pm 0.039)\%$ , obtained assuming leptonic universality in the charged weak current (42), the predicted branching ratio is

$$\mathcal{B}_{\text{CVC}}(\tau^- \rightarrow \nu_\tau \pi^- \pi^0) = (24.52 \pm 0.26_{\text{exp}} \pm 0.11_{\text{rad}} \pm 0.12_{\text{SU}(2)})\%. \quad 29.$$

The errors quoted are split into uncertainties from the experimental input (the  $e^+e^-$  annihilation cross sections) and the numerical integration procedure, the missing radiative corrections applied to the relevant  $e^+e^-$  data, and the isospin-breaking corrections when relating  $\tau$  and  $e^+e^-$  spectral function. The result in Equation 29 disagrees with the direct measurement,

$$\mathcal{B}_{\text{exp}}(\tau^- \rightarrow \nu_\tau \pi^- \pi^0) = (25.46 \pm 0.10)\%. \quad 30.$$

Even though the revised CMD-2 results have reduced the discrepancy between Equation 29 and the measurement from 4.6 to 2.9 standard deviations (adding all errors in quadrature), the remaining difference of  $[-0.94 \pm 0.10_\tau \pm$

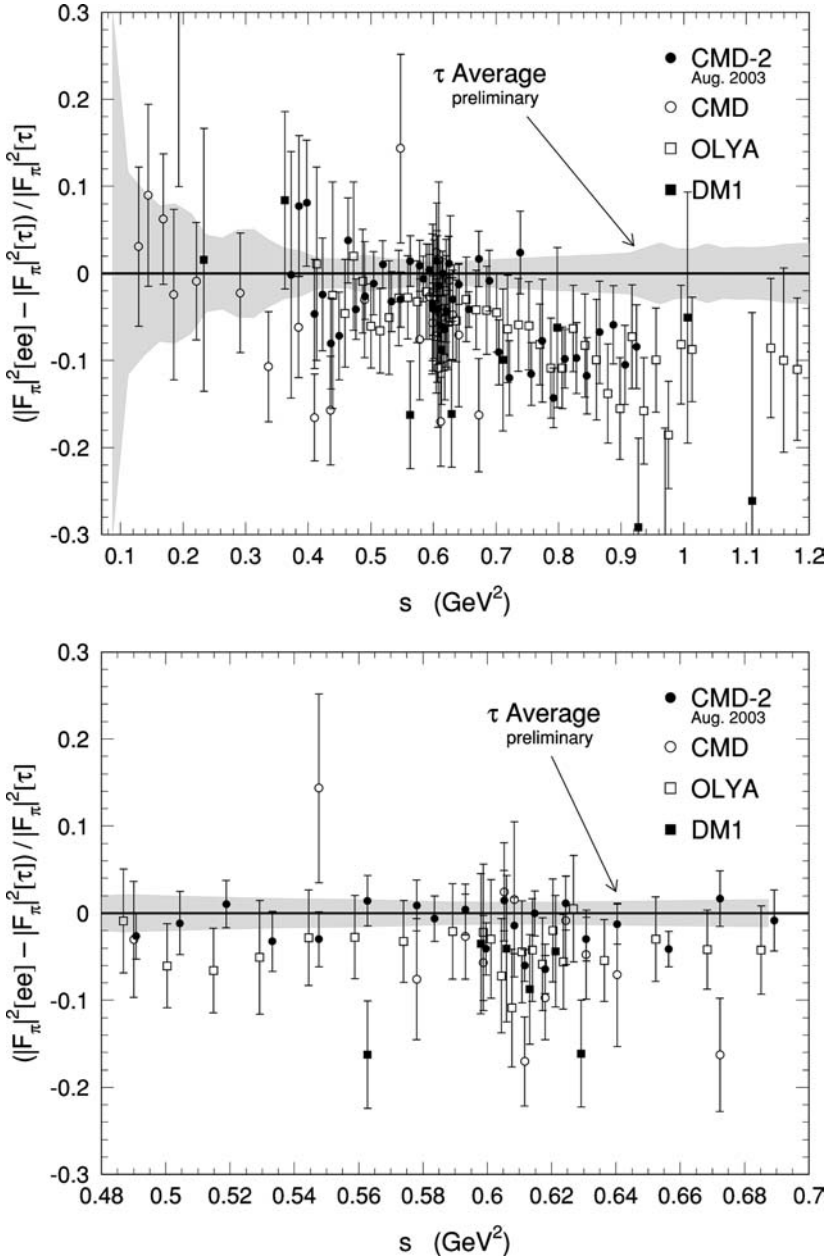


**Figure 5** Relative comparison of the  $\pi^+\pi^-$  spectral function from  $e^+e^-$  and isospin-breaking corrected  $\tau$  data, expressed as a ratio to the  $\tau$  spectral function. The band shows the uncertainty on the latter. The  $e^+e^-$  data are from CMD-2 (33), CMD (54), OLYA (54, 55), and DM1 (56). The bottom plot is an enlargement of the  $\rho$  region.

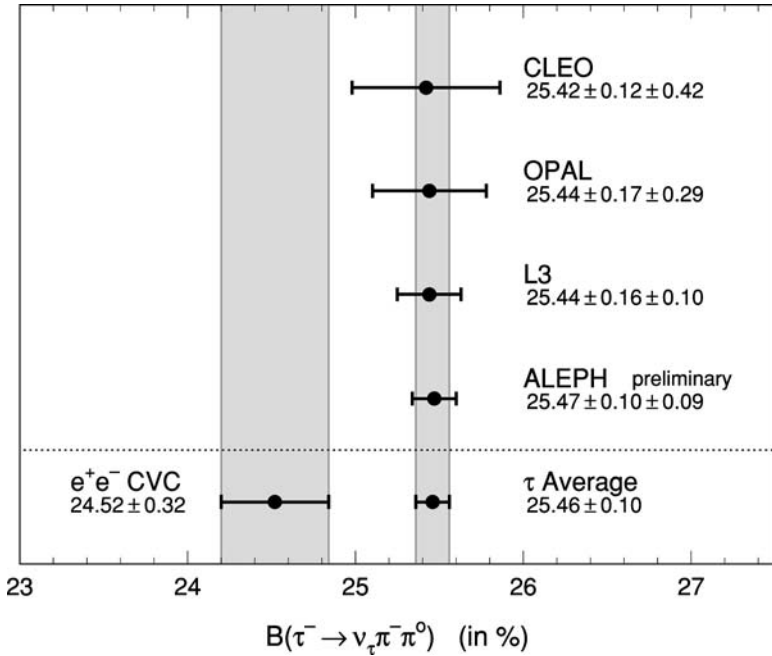


**Figure 6** The measured branching ratios for  $\tau^- \rightarrow \nu_\tau \pi^- \pi^0$  are compared to the prediction from the  $e^+e^- \rightarrow \pi^+\pi^-$  spectral function, applying the isospin-breaking correction factors discussed in Reference (32). The measured branching ratios are from ALEPH (42), CLEO (58), L3 (59), and OPAL (60). The L3 and OPAL results are obtained from their  $h\pi^0$  branching ratio, reduced by the small  $K\pi^0$  contribution measured by ALEPH (61) and CLEO (62).

$0.26_{\text{ee}} \pm 0.11_{\text{rad}} \pm 0.12_{\text{SU}(2)} (\pm 0.32_{\text{total}})]\%$  is still problematic. Since the disagreement between  $e^+e^-$  and  $\tau$  spectral function is more pronounced at energies above 850 MeV, we expect a smaller discrepancy in the calculation of  $a_\mu^{\text{had,LO}}$  because of the steeply falling function  $K(s)$ . More information on the comparison is displayed in Figure 6, where it is clear that ALEPH, CLEO, L3, and OPAL all separately, but with different significance, disagree with the  $e^+e^-$ -based CVC result.

The discrepancy between  $e^+e^-$  and  $\tau$  spectral function prevents us from presenting a unique evaluation of the dispersion integral that profits from both sources. On the one hand, it is clear that  $e^+e^-$  data are the natural input and that  $\tau$  data need additional treatment to cope with isospin-breaking corrections. On the other hand, recent history has taught us that the reliability of the input data is an important concern and therefore redundancy is needed. This is achieved within the  $\tau$  data sets, but not yet with  $e^+e^-$  data because it relies on only one precise experiment. The forthcoming results from KLOE (63) and BABAR (64) are very important to assess the consistency of the  $e^+e^-$  input.

## 4.5. Special Cases

4.5.1. THE THRESHOLD REGION To overcome the lack of precise data at threshold energies and to benefit from the analyticity property of the pion form factor, a third-order expansion in  $s$  is used:

$$F_{\pi}^0 = 1 + \frac{1}{6} \langle r^2 \rangle_{\pi} s + c_1 s^2 + c_2 s^3 + O(s^4). \quad 31.$$

Exploiting precise results from space-like data (65), we constrain the pion-charge radius-squared to  $\langle r^2 \rangle_{\pi} = (0.439 \pm 0.008) \text{ fm}^2$  and fit the two parameters  $c_{1,2}$  to the data in the range  $[2m_{\pi}, 0.6 \text{ GeV}]$ . Good agreement is observed in the low-energy region, where the expansion should be reliable. Since the fits incorporate unquestionable constraints from first principles, we use this parameterization for evaluating the integrals in the range up to 0.5 GeV.

4.5.2. QCD FOR THE HIGH-ENERGY CONTRIBUTIONS Because problems still remain regarding the spectral function from low-energy data, a conservative choice of using the QCD prediction only above an energy of 5 GeV is adopted. The details of the calculation can be found in References (26, 29) and in the references therein.

The perturbative QCD prediction uses a next-to-next-to-leading order  $O(\alpha_s^3)$  expansion of the Adler  $D$ -function (66), with second-order quark mass corrections (67).  $R(s)$  is obtained by numerical evaluation of a contour integral in the complex  $s$  plane. Nonperturbative effects are considered through the operator product expansion, giving power corrections controlled by gluon and quark condensates. The value  $\alpha_s(M_Z^2) = 0.1193 \pm 0.0026$ , used for the evaluation of the perturbative part, is taken as the average of the results from the analyses of  $\tau$  decays (68) and of the  $Z$  width in the global electroweak fit (69). The two determinations have comparable uncertainties (mostly theoretical for the  $\tau$  and experimental for the  $Z$ ) and agree well with each other. Uncertainties are taken to be equal to the common error on  $\alpha_s(M_Z^2)$ , to half of the quark mass corrections and to the full nonperturbative contributions. The QCD prediction is testable in the energy range between 1.8 and 3.7 GeV. The contribution to  $a_{\mu}^{\text{had,LO}}$  in this region is computed as  $(338.7 \pm 4.6) 10^{-11}$  using QCD, to be compared with the result of  $(349 \pm 18) 10^{-11}$  from the data. The two values agree within the 5% accuracy of the measurements.

Reference (29) showed that the evaluation of  $a_{\mu}^{\text{had,LO}}$  was improved by applying QCD sum rules. We do not consider this possibility here for the following two reasons. First, it is clear that the main problem at energies below 2 GeV is now the inconsistency between the  $e^+e^-$  and  $\tau$  input data, and resolving this is a more urgent priority. Second, the improvement provided by the use of QCD sum rules results from a balance between the experimental accuracy of the data and the theoretical uncertainties. The present precision of both  $e^+e^-$  and  $\tau$  data, should they agree, is such that the gain would be smaller than before.



## 4.6. Results for the Leading-Order Hadronic Vacuum Polarization

Figure 7 gives a panoramic view of the  $e^+e^-$  data in the relevant energy range. The cross-hatched band indicates the QCD prediction, which is used here only for energies above 5 GeV. Note that the plotting of the QCD band takes into account the thresholds for open-flavor  $B$  states, in order to facilitate the comparison with the data in the continuum. However, for the evaluation of the integral, the  $b\bar{b}$  threshold

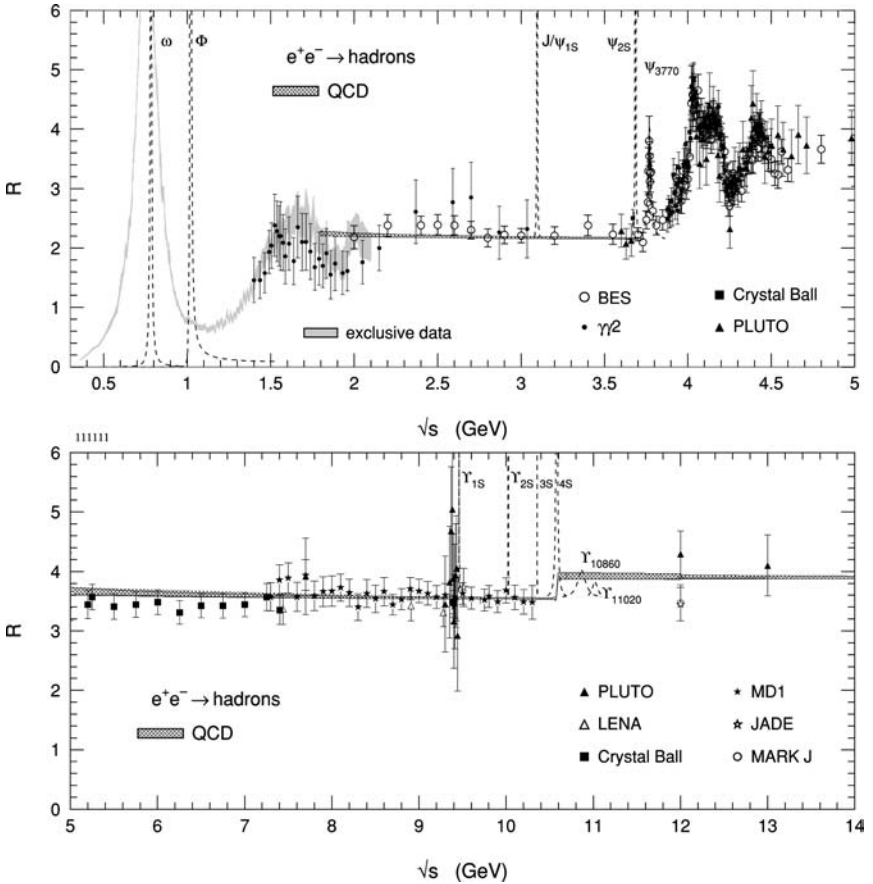


**Figure 7** Compilation of the data contributing to  $a_{\mu}^{\text{had,LO}}$ . Shown is the total hadronic-over-muonic cross-section ratio  $R$ . The shaded band below 2 GeV represents the sum of the exclusive channels considered in this analysis, except for the contributions from the narrow resonances, which are indicated by dashed lines. All data points shown correspond to inclusive measurements. The cross-hatched band gives the prediction from (essentially) perturbative QCD (see text).

is taken at twice the pole mass of the  $b$  quark, so that the contribution includes the narrow  $\Upsilon$  resonances, according to global quark-hadron duality.

The discrepancies discussed above are now expressed directly in terms of  $a_\mu^{\text{had,LO}}$ . The resulting estimates for the  $e^+e^-$ -based data set are smaller by  $(-119 \pm 73) 10^{-11}$  for the  $\pi\pi$  channel and  $(-28 \pm 29) 10^{-11}$  for the sum of the  $4\pi$  channels. The total difference  $(-147 \pm 79) 10^{-11}$  could now be considered acceptable, but the systematic difference between the  $e^+e^-$  and  $\tau\pi\pi$  spectral function at high energies precludes a straightforward combination of the two evaluations.

The results for the lowest-order hadronic contribution are

$$\begin{aligned} a_\mu^{\text{had,LO}} &= (6963 \pm 62_{\text{exp}} \pm 36_{\text{rad}}) 10^{-11} && [\text{DEHZ}e^+e^-\text{-based}], \\ a_\mu^{\text{had,LO}} &= (7110 \pm 50_{\text{exp}} \pm 8_{\text{rad}} \pm 28_{\text{SU}(2)}) 10^{-11} && [\text{DEHZ}\tau\text{-based}]. \end{aligned} \quad 32.$$

#### 4.7. Comparison of Different Analyses

As we have mentioned, it only makes sense to compare estimates based on the same input data, considering the recent significant correction of the CMD-2 data (33). Besides the approach described above using both  $e^+e^-$  and  $\tau$  spectral function two other determinations are available.

The Hagiwara-Martin-Nomura-Teubner (HMNT) calculation (70) also uses the complete set of available exclusive channels up to 1.4 GeV, but only inclusive measurements above. The two main differences between this estimate and the one described are the treatment of data in the threshold region and the use of inclusive data between 1.4 and 2 GeV. In both cases, the results are consistent within the experimental errors, but the analysis (70) yields lower central values with a more aggressive theoretical error.

It is difficult to comment on the second determination, by Ghozzi & Jegerlehner (GJ) (50), because the authors provide no information about the data used, the way they are handled, and the different contributions to the final error. The values found,

$$\begin{aligned} a_\mu^{\text{had,LO}} &= (6961.5 \pm 57_{\text{exp}} \pm 24_{\text{rad}}) 10^{-11} && [\text{HMNT exclusive (70)}], \\ a_\mu^{\text{had,LO}} &= (6948 \pm 86) 10^{-11} && [\text{GJ (50)}], \end{aligned} \quad 33.$$

are in agreement with the  $e^+e^-$ -based result that was found in the DEHZ analysis and is quoted in Equation 32. Although the experimental errors should be strongly correlated, differences between the analyses could result from the treatment of experimental systematic uncertainties, the numerical integration procedure (which may involve the averaging of neighboring data points), and the treatment of missing radiative corrections.

The value determined by HMNT using the inclusive  $e^+e^-$  data between 1.4 and 2 GeV is consistent with the exclusive analysis within one standard deviation (computed with respect to the respective inclusive-exclusive uncertainties in the 1.4–2 GeV range). However, it turns out to be somewhat smaller:

$$a_\mu^{\text{had,LO}} = (6924 \pm 59_{\text{exp}} \pm 24_{\text{rad}}) 10^{-11} \quad [\text{HMNT inclusive (70)}]. \quad 34.$$

Since the  $e^+e^-$  exclusive and inclusive predictions agree within errors, we combine them into a single mean value, using the more conservative error estimate,

$$a_\mu^{\text{had,LO}} = (6944 \pm 62_{\text{had,LO}} \pm 36_{\text{rad}}) 10^{-11} \quad [e^+e^- \text{ average}]. \quad 35.$$

## 5. HADRONIC THREE-LOOP EFFECTS

The three-loop hadronic contributions to  $a_\mu^{\text{SM}}$  involve one hadronic vacuum polarization insertion with an additional loop (either photonic or another leptonic or hadronic vacuum polarization insertion). They can be evaluated (71) using the same  $e^+e^- \rightarrow$  hadrons data sets described in Section 4. Calling that subset of  $\mathcal{O}(\alpha/\pi)^3$  hadronic contributions  $a_\mu^{\text{had,NLO}}$ , we quote here the result of a recent analysis (70),

$$a_\mu^{\text{had,NLO}} = -98(1) \times 10^{-11}, \quad 36.$$

which is consistent with results of earlier studies (30, 71). It would change by about  $-3 \times 10^{-11}$  if the  $\tau$  data described in Section 4 were used.

More controversial are the hadronic light-by-light (LBL) scattering contributions illustrated in Figure 8. A dispersion relation approach using data is not possible, and a first-principles calculation [e.g., using lattice gauge theory (72)] has not been carried out. Instead, calculations involving pole insertions, short-distance quark loops (73), and charged-pion loops have been individually performed in a large  $N_c$  QCD approach. The pseudoscalar poles ( $\pi^\circ$ ,  $\eta$ , and  $\eta'$ ) dominate such a calculation. Unfortunately, in early studies the sign of their contribution was

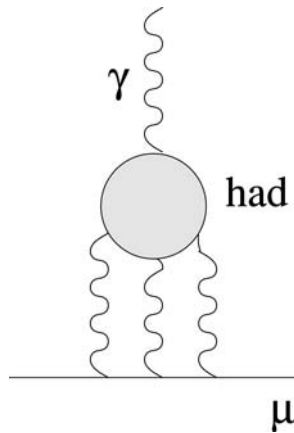


**Figure 8** The hadronic light-by-light scattering contribution.

incorrect and misleading. Its correction (74) led to a large shift in the  $a_\mu^{\text{SM}}$  prediction. A representative estimate (32) of the LBL contribution, which includes  $\pi$ ,  $\eta$ , and  $\eta'$  poles as well as other resonances, charged pion loops, and quark loops, currently gives

$$a_\mu^{\text{had,LBL}} \simeq 86(35) \times 10^{-11} \quad [\text{representative}]. \quad 37.$$

Recently, however, Melnikov & Vainshtein (MV) published a new analysis of LBL (75). Their approach for the first time properly matches the asymptotic short-distance behavior of pseudoscalar and axial-vector contributions with the free quark-loop behavior. It yields the somewhat larger result

$$a_\mu^{\text{had,LBL}} = 136(25) \times 10^{-11} \quad [\text{MV (75)}]. \quad 38.$$

The MV analysis excluded several small and (probably) negative contributions, such as charged pion loops and scalar resonances. These could reduce the magnitude of the result in Equation 38, but probably not too significantly. In fact, Melnikov & Vainshtein provide a consistency check on their result in the spirit of the electroweak hadronic triangle diagram study (19, 76) discussed in Section 3. They combine constituent quark masses in the LBL diagram with a pion-pole contribution that properly accounts for the chiral properties of massless QED and avoids short-distance double counting. They find  $a_\mu^{\text{had,LBL}} \simeq 120 \times 10^{-11}$ , with about half of the contribution coming from quark diagrams and the other half from the pion pole. We employ that result along with a rather conservative error that we assigned so that the results in Equations 37 and 38 overlap within their errors:

$$a_\mu^{\text{had,LBL}} \simeq 120(35) \times 10^{-11}. \quad 39.$$

Further resolution of the LBL contribution is very important. At present, we use the result in Equation 39 for comparison with experiment. We find from Equations 36 and 39

$$a_\mu^{\text{had,3-loop}} = 22(35) \times 10^{-11}. \quad 40.$$

That value is reduced by about  $3 \times 10^{-11}$  if  $\tau$  data are used.

## 6. COMPARISON OF THEORY AND EXPERIMENT

By collecting the results from previous sections on  $a_\mu^{\text{QED}}$ ,  $a_\mu^{\text{EW}}$ ,  $a_\mu^{\text{had,LO}}$ ,  $a_\mu^{\text{had,NLO}}$ , and  $a_\mu^{\text{had,LBL}}$ , we can obtain the standard-model prediction for  $a_\mu$ . Because the situation on  $a_\mu^{\text{had,LO}}$  is not yet settled, we must quote two values using the  $e^+e^-$  (31, 50, 70) and the  $\tau$  decay data (31),

$$\begin{aligned} a_\mu^{\text{SM}} &= (116591841 \pm 72_{\text{had,LO}} \pm 35_{\text{LBL}} \pm 3_{\text{QED+EW}}) 10^{-11} [e^+e^-], \\ a_\mu^{\text{SM}} &= (116592004 \pm 58_{\text{had,LO}} \pm 35_{\text{LBL}} \pm 3_{\text{QED+EW}}) 10^{-11} [\tau]. \end{aligned} \quad 41.$$

The standard-model values can be compared to the measurement (13). Keeping experimental and theoretical errors separate, we find the following differences between measured and predicted values,  $\Delta a_\mu = a_\mu^{\text{exp}} - a_\mu^{\text{SM}}$ :

$$\begin{aligned} \Delta a_\mu &= (239 \pm 72_{\text{had,LO}} \pm 35_{\text{other}} \pm 58_{\text{exp}}) 10^{-11} [e^+e^-], \\ \Delta a_\mu &= (76 \pm 58_{\text{had,LO}} \pm 35_{\text{other}} \pm 58_{\text{exp}}) 10^{-11} [\tau], \end{aligned} \tag{42}$$

where the first error quoted is specific to each approach, the second is due to contributions other than hadronic vacuum polarization, and the third is the Brookhaven g-2 experimental error. The last two errors are identical in both evaluations. With all errors added in quadrature, the differences in Equation 42 correspond to 2.4 and 0.9 standard deviations, respectively. Figure 9 provides a graphical comparison of the results with the experimental value. A word of caution is in order about the real meaning of “standard deviations,” as the uncertainty in the theoretical prediction is dominated by systematic errors in the  $e^+e^-$  experiments for which a gaussian distribution is questionable.

At this point we repeat that the  $e^+e^-$ -based estimate is the most direct one and should in general be preferred. However, because the  $e^+e^-$ - $\tau$  discrepancy is still unresolved and the  $e^+e^-$  results rely on only one precise experiment, we find it appropriate to keep in mind the  $\tau$ -based estimate.

The apparent deviation from the  $e^+e^-$ -based prediction is of great interest, even if it is not an overwhelming discrepancy. Ordinarily, one would not necessarily worry about a 2.4  $\sigma$  effect. In fact, the proper response would be to improve the

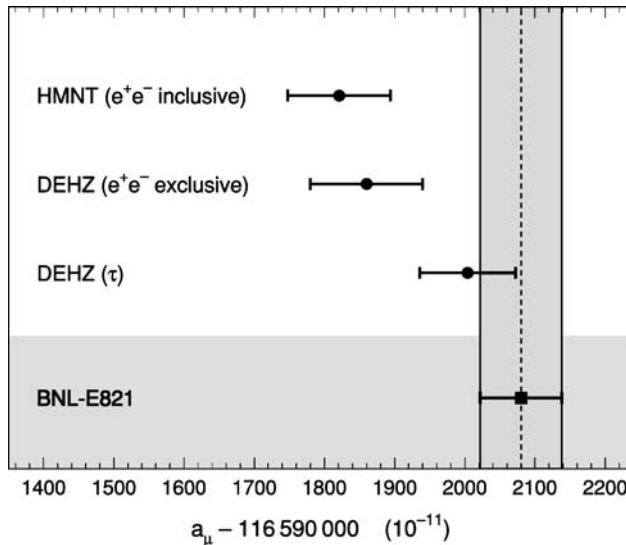


**Figure 9** Comparison of the theoretical estimates (31, 70) with the Brookhaven measurement (13).

experimental measurement (which is statistics-limited) by further running and to continue to improve the theory. With regard to the latter, new  $e^+e^- \rightarrow$  hadrons data and further study of LBL could potentially reduce the overall theoretical uncertainty. The deviation observed in Equation 42 stirs excitement because a deviation of this magnitude could arise from new physics. In the next section, we briefly review several examples.

## 7. NEW-PHYSICS CONTRIBUTIONS

A deviation of about  $240 \times 10^{-11}$  in  $\Delta a_\mu = a_\mu^{\text{exp}} - a_\mu^{\text{SM}}$  would have interesting implications if truly due to new physics. The leading contender for causing such an effect is supersymmetry. Indeed, supersymmetric contributions to  $a_\mu$  can stem from sneutrino-chargino and smuon-neutralino loops, as illustrated in Figure 10. Those diagrams actually describe two-chargino and four-neutralino states and could include three-generation slepton mixing. In general, a broad range of predictions are possible depending on particle masses, couplings, etc. For illustration purposes, we assume degenerate masses  $\sim m_{\text{SUSY}}$  in all loops (77) (not a realistic assumption but one that should roughly approximate expectations). Then, in terms of  $\tan \beta = \langle \phi_2 \rangle / \langle \phi_1 \rangle$ , the ratio of Higgs vacuum expectations, and  $\text{sign}(\mu) = \pm$ , one finds (for  $\tan \beta \geq 3$ )  $a_\mu^{\text{SUSY}} \simeq \text{sign}(\mu) \times 130 \times 10^{-11} (100 \text{ GeV}/m_{\text{SUSY}})^2 \tan \beta$ , where two-loop leading-log QED suppression effects have been included (12). Equating that prediction with a  $+240 \times 10^{-11}$  deviation suggests  $\text{sign}(\mu) = +$  and  $m_{\text{SUSY}} \simeq 74 \sqrt{\tan \beta} \text{ GeV}$ .

The  $\text{sign}(\mu) = +$  scenario is also favored by  $b \rightarrow s\gamma$  data, while for  $3 \leq \tan \beta \leq 40$  the range  $127 \text{ GeV} \leq m_{\text{SUSY}} \leq 465 \text{ GeV}$  is in keeping with expectations of supersymmetry enthusiasts. So, a deviation in  $\Delta a_\mu$  of about the apparent magnitude is a relatively generic prediction of low-mass supersymmetry models. If supersymmetry is eventually discovered at high-energy colliders and the masses measured, it will be possible to use  $\Delta a_\mu$  to determine  $\tan \beta$ .

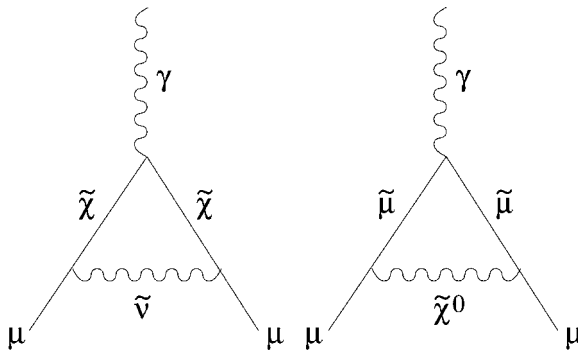


**Figure 10** Two contributions from lowest-order supersymmetry.

Another generic possibility (78) is new physics related to the origin of the muon mass via loop effects (radiative muon mass scenarios). In such schemes (12), the muon mass originates from a chiral-symmetry-breaking loop effect. The corresponding high-scale  $M$  can arise from dynamics, extra dimensions, multi-Higgs, softly broken supersymmetry, etc. One finds generically  $a_\mu(M) \simeq C(m_\mu^2/M^2)$ , where  $C$  is  $\mathcal{O}(1)$  rather than  $(\alpha/\pi)$ . A deviation of  $\Delta a_\mu \simeq 240 \times 10^{-11}$  corresponds to  $M \simeq 2$  TeV, an interesting possibility. Indeed, if supersymmetry is not found at high-energy colliders, it is highly likely that other  $\mathcal{O}(1$  TeV)-scale physics will emerge. If the  $\Delta a_\mu$  deviation is related, it would suggest that mass-generating new physics is at hand.

Other forms of new physics (12), such as  $Z'$  or  $W_R$  bosons and anomalous  $W$  dipole moments, generally lead to unobservably small  $\Delta a_\mu$ . So supersymmetry (with its relatively low mass scale and  $\tan \beta$  enhancement) and models with no  $\alpha/\pi$  suppression are the more natural candidates to explain a deviation from zero in  $\Delta a_\mu$ .

## 8. OUTLOOK

After considerable effort, the experiment E821 at Brookhaven has improved the determination of  $a_\mu$  by about a factor of 14 relative to the classic CERN results of the 1970s (79). The result is still statistics-limited and could be improved by another factor of two or so (to a precision of  $30 \times 10^{-11}$ ) before systematics effects become a limitation. Pushing the experiment to that level seems an obvious goal for the near term. In the longer term, a new experiment with improved muon acceptance and magnetic fields could potentially reach  $6 \times 10^{-11}$  (80).

The theoretical prediction within the standard model is a more immediate limitation. The current  $80 \times 10^{-11}$  error is dominated by uncertainties in  $e^+e^- \rightarrow$  hadrons that lead to a  $\sim 1\%$  error in the evaluation of the hadronic vacuum polarization contribution. This estimate so far relies primarily on only one precise experiment, so redundancy is very desirable. Data obtained with a different technique, such as the radiative return process  $e^+e^- \rightarrow \gamma +$  hadrons (63, 64), will provide a consistency check and could lead to a reduction of the error. Progress is also needed in the development of cross-checked Monte Carlo programs to apply radiative corrections with an increased confidence. The  $\tau$  results, which currently disagree with the available  $e^+e^-$  results, should be reviewed after consolidation of the  $e^+e^-$  data with reconsideration of the isospin-breaking corrections. Finally, lattice gauge theories with dynamical fermions (72) can in principle provide a determination of  $a_\mu^{\text{had,LO}}$ . All sources considered, and assuming all discrepancies to be resolved, it appears difficult to reach an uncertainty much better than  $35 \times 10^{-11}$  in this sector.

The 30% uncertainty in hadronic LBL contributions ( $35 \times 10^{-11}$ ) is largely model-dependent. Here one could imagine that further work following the MV approach (75) or a lattice calculation could reduce the error by a factor of two.

Doing much better appears to be difficult, but such an improvement would be well matched to short-term experimental capabilities.

If the above experimental and theoretical improvements do occur, they will lead to a total uncertainty in  $\Delta a_\mu = a_\mu^{\text{exp}} - a_\mu^{\text{SM}}$  of about  $50 \times 10^{-11}$ , i.e., half the current uncertainty. This would provide a very important step in testing the standard model, particularly if the current difference persists, since it would translate to a  $\sim 5\sigma$  discrepancy. The result could be used in conjunction with future collider discoveries to sort out the properties of new physics (e.g., the size of  $\tan\beta$  in supersymmetry) or constrain further possible appendages to the standard model.

## ACKNOWLEDGMENTS

We thank the many colleagues who contributed to this exciting field.

**The Annual Review of Nuclear and Particle Science is online at  
<http://nucl.annualreviews.org>**

## LITERATURE CITED

1. Dirac PAM. *Proc. R. Soc.* A117:610 (1928)
2. Schwinger J. *Phys. Rev.* 73:416L (1948)
3. Nagle J, Nelson E, Rabi I. *Phys. Rev.* 71:914 (1947); Nagle J, Julian R, Zacharias J. *Phys. Rev.* 72:971 (1947)
4. van Dyck RS, Schwinger PB, Dehmelt HG. *Phys. Rev. Lett.* 59:26 (1987)
5. Kinoshita T, Nio M. *Phys. Rev. Lett.* 90:021803 (2003)
6. Laporta S, Remiddi E. *Phys. Lett.* B379: 283 (1996)
7. Czarnecki A, Marciano W. *Nucl. Phys. B Proc.* 76:245 (1999)
8. Marciano W. In *Proc. Dirac Centennial Symp.* Singapore: World Sci. (2002)
9. Mohr P, Taylor B. *Rev. Mod. Phys.* 72:351 (2000)
10. Gabrielse G, Tan J. In *Cavity Quantum Electrodynamics*, ed. P Berman, p. 267. San Diego: Academic (1994)
11. Kinoshita T. In *The Gregory Breit Centennial Symposium*, ed. V Hughes, F Iachello, D Kusnizov. Singapore: World Sci. (2001)
12. Czarnecki A, Marciano W. *Phys. Rev. D* 64:013014 (2001)
13. Bennett GW, et al. (E821 g-2 Collab.) *Phys. Rev. Lett.* 89:101804 (2002); hep-ex/0401008
14. Kinoshita T, Nio M. hep-ph/0402206
15. Czarnecki A, Krause B, Marciano W. *Phys. Rev. D* 52:2619 (1995); *Phys. Rev. Lett.* 76:3267 (1996)
16. Kinoshita T, Nizic B, Okamoto Y. *Phys. Rev. D* 41:593 (1990); Milstein AI, Yelkhovskiy AS. *Phys. Lett.* B233:11 (1989); Karshenboim SG. *Phys. Atom. Nucl.* 56: 857 (1993); Kataev AL, Starshenko VV. *Phys. Rev. D* 52:402 (1995)
17. Jackiw R, Weinberg S. *Phys. Rev. D* 5:2396 (1972); Altarelli G, Cabibbo N, Maiani L. *Phys. Lett.* B40:415 (1972); Bars I, Yoshimura M. *Phys. Rev. D* 6:374 (1972); Fujikawa K, Lee BW, Sanda AI. *Phys. Rev. D* 6:2923 (1972)
18. Kukhto T, Kuraev EA, Schiller A, Silagadze ZK. *Nucl. Phys. B* 371:567 (1992)
19. Czarnecki A, Marciano W, Vainshtein A. *Phys. Rev. D* 67:073006 (2003)
20. Degrassi G, Giudice GF. *Phys. Rev. D* 58:053007 (1998)
21. Adler SL. *Phys. Rev.* 177:2426 (1969); Bell J, Jackiw R. *Nuovo Cim.* A60:47 (1969)



22. Peris S, Perrottet M, de Rafael E. *Phys. Lett.* B355:523 (1995); Knecht M, et al. *JHEP* 0211:003 (2002)
23. Gourdin M, de Rafael E. *Nucl. Phys. B* 10:667 (1969)
24. Brodsky SJ, de Rafael E. *Phys. Rev.* 168:1620 (1968)
25. Martin AD, Zeppenfeld D. *Phys. Lett.* B345:558 (1995)
26. Davier M, Höcker A. *Phys. Lett.* B419:419 (1998)
27. Kühn JH, Steinhauser M. *Phys. Lett.* B437:425 (1998)
28. Groote S, et al. *Phys. Lett.* B440:375 (1998)
29. Davier M, Höcker A. *Phys. Lett.* B435:427 (1998)
30. Alemany R, Davier M, Höcker A. *Eur. Phys. J. C* 2:123 (1998)
31. Davier M, Eidelman S, Höcker A, Zhang Z. *Eur. Phys. J. C* 31:503 (2003)
32. Davier M, Eidelman S, Höcker A, Zhang Z. *Eur. Phys. J. C* 27:497 (2003)
33. Akhmetshin R, et al. (CMD-2 Collab.) hep-ex/0308008
34. Bonneau G, Martin F. *Nucl. Phys. B* 27:381 (1971)
35. Eidelman S, Kuraev E. *Phys. Lett.* B80:94 (1978)
36. Swartz ML. *Phys. Rev. D* 53:5268 (1996)
37. Höfer A, Gluza J, Jegerlehner F. *Eur. Phys. J. C* 24:51 (2002)
38. Barate R, et al. (ALEPH Collab.) *Z. Phys. C* 76:15 (1997)
39. Anderson S, et al. (CLEO Collab.) *Phys. Rev. D* 61:112002 (2000)
40. Edwards KW, et al. (CLEO Collab.) *Phys. Rev. D* 61:072003 (2000)
41. Ackerstaff K, et al. (OPAL Collab.) *Eur. Phys. J. C* 7:571 (1999)
42. ALEPH Collab. ALEPH 2002-030 CONF 2002-019 (July 2002)
43. Tsai P. *Phys. Rev. D* 4:2821 (1971)
44. Hagiwara K, et al. *Phys. Rev. D* 66:010001 (2002)
45. Marciano WJ, Sirlin A. *Phys. Rev. Lett.* 61:1815 (1988)
46. Sirlin A. *Nucl. Phys. B* 196:83 (1982)
47. Braaten E, Narison S, Pich A. *Nucl. Phys. B* 373:581 (1992)
48. Czyż H, Kühn JH. *Eur. Phys. J. C* 18:497 (2001)
49. Davier M. *Spectral functions from hadronic  $\tau$  decays*. Workshop on  $e^+e^-$  Hadronic Cross Section, Pisa, Oct. 8–10 (2003), hep-ex/0312064
50. Ghozzi S, Jegerlehner F. hep-ph/0310181
51. Singer P. *Phys. Rev.* 130:2441 (1963); erratum, *Phys. Rev.* 161:1694 (1967)
52. Cirigliano V, Ecker G, Neufeld H. *Phys. Lett.* B513:361 (2001)
53. Cirigliano V, Ecker G, Neufeld H. *JHEP* 0208:002 (2002)
54. Barkov LM, et al. (OLYA, CMD Collab.) *Nucl. Phys. B* 256:365 (1985)
55. Vasserman IB, et al. (OLYA Collab.) *Sov. J. Nucl. Phys.* 30:518 (1979)
56. Quenzer A, et al. (DM1 Collab.) *Phys. Lett.* B76: 512 (1978)
57. Davier M. *Updated estimate of the muon magnetic moment using revised results from  $e^+e^-$  annihilation*. Workshop on  $e^+e^-$  Hadronic Cross Section, Pisa, Oct. 8–10 (2003), hep-ex/0312065
58. Artuso M, et al. (CLEO Collab.) *Phys. Rev. Lett.* 72:3762 (1994)
59. Achard P, et al. (L3 Collab.) CERN-EP/2003-019, May 2003
60. Ackerstaff K, et al. (OPAL Collab.) *Eur. Phys. J. C* 4:93 (1998)
61. Barate R, et al. (ALEPH Collab.) *Eur. Phys. J. C* 11:599 (1999)
62. Battle M, et al. (CLEO Collab.) *Phys. Rev. Lett.* 73:1079 (1994)
63. Valeriani B. *Preliminary results from KLOE on the radiative return*. Workshop on  $e^+e^-$  Hadronic Cross Section, Pisa, Oct. 8–10 (2003)
64. Davier M. *Status of the BaBar  $R$  measurement using radiative return*. Workshop on  $e^+e^-$  Hadronic Cross Section, Pisa, Oct. 8–10 (2003), hep-ex/0312093
65. Amendolia SR, et al. (NA7 Collab.) *Nucl. Phys. B* 277:168 (1986)
66. Surguladze LR, Samuel MA. *Phys. Rev. Lett.* 66:560 (1991); Gorishny SG, Kataev

- KL, Larin SA. *Phys. Lett.* B259:144 (1991)
67. Chetyrkin KG, Kühn JH, Steinhauser M. *Nucl. Phys. B* 482:213 (1996)
68. Barate R, et al. (ALEPH Collab.) *Eur. J. Phys. C* 4:409 (1998)
69. LEP Electroweak Work. Group. LEPE-WWG/2002-01, May 2002
70. Hagiwara K, Martin AD, Nomura D, Teubner T. hep-ph/0312250
71. Krause B. *Phys. Lett.* B390:392 (1997)
72. Blum T. *Phys. Rev. Lett.* 91:052001 (2003)
73. Hayakawa M, Kinoshita T. *Phys. Rev. D* 57:465 (1998); Bijnens J, Pallante E, Prades J. *Nucl. Phys. B* 474:379 (1996)
74. Knecht M, Nyffeler A. *Phys. Rev. D* 65:073034 (2002); Knecht M, et al. *Phys. Rev. Lett.* 88:071802 (2002); Blokland I, Czarnecki A, Melnikov K. *Phys. Rev. Lett.* 88:071803 (2002); Hayakawa M, Kinoshita K. Erratum, *Phys. Rev. D* 66:019902 (2002); Bijnens J, Pallante E, Prades J. *Nucl. Phys. B* 626:410 (2002)
75. Melnikov K, Vainshtein A. hep-ph/0312226
76. Vainshtein A. *Phys. Lett.* B569:187 (2003)
77. Moroi T. *Phys. Rev. D* 53:6565 (1996); erratum, *Phys. Rev. D* 56:4424 (1997); Ibrahim T, Nath P. *Phys. Rev. D* 57:478 (1998); Kosower D, Krauss L, Sakai N. *Phys. Lett.* B133:305 (1983)
78. Marciano W. In *Particle Theory and Phenomenology*, ed. K Lassila, et al., p. 22. Singapore: World Sci. (1996); *Radiative Corrections Status and Outlook*, ed. BFL Ward, p. 403. World Sci. (1995)
79. Bailey J, et al. *Phys. Lett.* B68:191 (1977); Farley FJM, Picasso E. *The muon (g-2) Experiments. Advanced Series on Directions in High Energy Physics—Vol. 7. Quantum Electrodynamics*, ed. T Kinoshita. Singapore: World Sci. (1990)
80. Roberts BL. In *High Intensity Muon Sources*, ed. Y Kuno, T Yokoi, p. 69. Singapore: World Sci. (1999)

## CONTENTS

---

FRONTISPIECE, <i>Lincoln Wolfenstein</i>	xii
THE STRENGTH OF THE WEAK INTERACTIONS, <i>Lincoln Wolfenstein</i>	1
THE SOLAR <i>hep</i> PROCESS, <i>Kuniharu Kubodera and Tae-Sun Park</i>	19
TRACING NOBLE GAS RADIONUCLIDES IN THE ENVIRONMENT, <i>Philippe Collon, Walter Kutschera, and Zheng-Tian Lu</i>	39
THE GERASIMOV-DRELL-HEARN SUM RULE AND THE SPIN STRUCTURE OF THE NUCLEON, <i>Dieter Drechsel and Lothar Tiator</i>	69
THE THEORETICAL PREDICTION FOR THE MUON ANOMALOUS MAGNETIC MOMENT, <i>Michel Davier and William J. Marciano</i>	115
THE BROOKHAVEN MUON ANOMALOUS MAGNETIC MOMENT EXPERIMENT, <i>David W. Hertzog and William M. Morse</i>	141
THE NUCLEAR STRUCTURE OF HEAVY-ACTINIDE AND TRANSACTINIDE NUCLEI, <i>M. Leino and F.P. Heßberger</i>	175
ELECTROMAGNETIC FORM FACTORS OF THE NUCLEON AND COMPTON SCATTERING, <i>Charles Earl Hyde-Wright and Kees de Jager</i>	217
PHYSICS OPPORTUNITIES WITH A TEV LINEAR COLLIDER, <i>Sally Dawson and Mark Oreglia</i>	269
DIRECT DETECTION OF DARK MATTER, <i>Richard J. Gaitskell</i>	315
BACKGROUNDS TO SENSITIVE EXPERIMENTS UNDERGROUND, <i>Joseph A. Formaggio and C.J. Martoff</i>	361
GENERALIZED PARTON DISTRIBUTIONS, <i>Xiangdong Ji</i>	413
HEAVY QUARKS ON THE LATTICE, <i>Shoji Hashimoto and Tetsuya Onogi</i>	451
THE GRIBOV CONCEPTION OF QUANTUM CHROMODYNAMICS, <i>Yuri L. Dokshitzer and Dmitri E. Kharzeev</i>	487
GRAVITATIONAL WAVE ASTRONOMY, <i>Jordan B. Camp and Neil J. Cornish</i>	525

## INDEXES

Cumulative Index of Contributing Authors, Volumes 45–54	579
Cumulative Index of Chapter Titles, Volumes 45–54	582

## ERRATA

An online log of corrections to *Annual Review of Nuclear and Particle Science* chapters may be found at  
<http://nucl.annualreviews.org/errata.shtml>